Q DETERMINATION OF TRANSMISSION GPR WAVES IN ABSORBING MEDIA

by Eddy Ibrahim

Review of Information Engineering and Applications
2015 Vol. 2, No. 2, 33-50.
ISSN(e): 2409-6539
ISSN(p): 2412-3676
DOI: 10.18488/journal.79/2015.2.2/79.2.33.50

Q DETERMINATION OF TRANSMISSION GPR WAVES IN ABSORBING MEDIA

Eddy Ibrahim[1]+ --- **Wahyudi W.Parnadi**[2]
[1]*Department of Mining Engineering, University of Sriwijaya, Palembang, Indonesia*
[2]*Department of Geophysical Science & Engineering, Institute Technology Bandung, Bandung, Indonesia*

ABSTRACT

The absorption of electromagnetic waves is the most important parameter for the processing and interpretation of Ground-Penetrating Radar (GPR) data. Both the phase velocity v and the absorption coefficient α are frequency-dependent. From the linear basis of the frequency dependence of α of geology media, a constant Q-hypothesis is valid, whereby the Q factor is inversely proportional to α and describes material-specific absorption. For the near-reality description of electromagnetic waves propagation in rocks, modeling with constant Q and velocity dispersion after Futterman is carried out. On the basis of such model, the effect of these parameters on wavelets is investigated. As a result of absorption, the wave amplitudes become smaller with increasing distance at the same Q and become smaller with decreasing Q at the same distance and the waveforms are stretched . The longer the distance at the same Q as well as the smaller Q at the same distance, the smaller is the bandwidth of the transmission wavelets. At the same time, its peak frequency moves toward smaller frequencies. In addition, three methods for the determination of the absorption through Q factor are reviewed, namely the spectral ratio method, amplitude decay method and a method over absorption coefficient determination. The applicability of the methods is then demonstrated by using real data acquired from transmission measurement at test site in Reiche Zeche Shaft in Germany.

Keywords: Absorption, Dispersion, Relaxation model, Q factor, Spectral ratio method, Amplitude decay method, Velocity, Frequency, GPR processing and interpretation.

Contribution/ Originality

The new analysis for the determination of the absorption media by attenuation through Q factor.

1. INTRODUCTION

During propagation in geology medium electromagnetic (EM) waves are influenced by absorption process. The process leads to a decrease in the wave energy. As a result of the

+ Corresponding author

attenuation the wave amplitude becomes lower with increasing distance (absorption) and in particular, due to strong frequency dependence of the absorption process, the wave is increasingly stretched (dispersion). Therefore EM waves become carrier of both structural and petro-physical information about the medium.

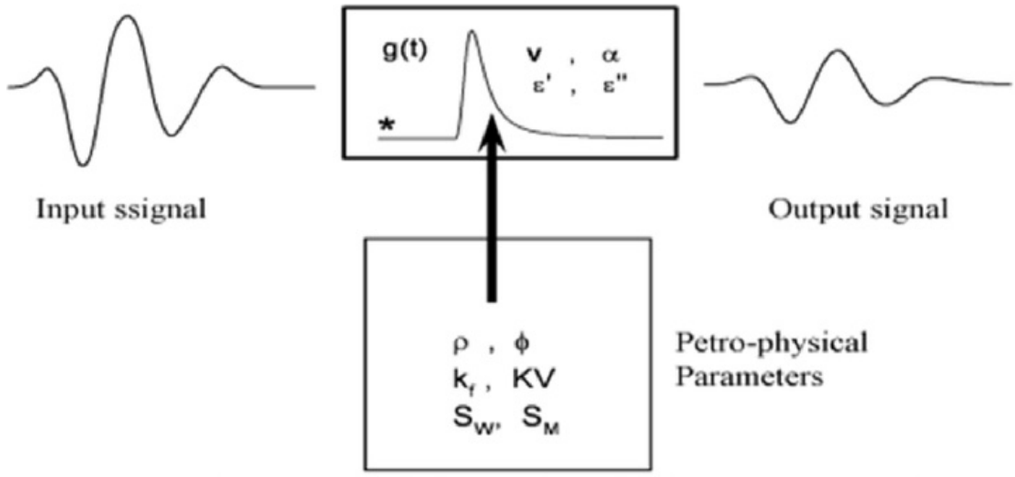

Figure-1. Illustration of physical cause and its effect in attenuated waves. * g(t) denote convolution with impulse response of absorbing medium.
(**Source:** Modified by the Researchers)

Figure 1 shows the attenuation of EM waves during their propagation in a medium. Physically the output signal results from a convolution of the input signal with corresponding impulse response of the medium. Wave propagation in the medium is described by two propagation parameters namely phase velocity v and absorption coefficient α or real part $\varepsilon_r^{'}$ and imaginary part $\varepsilon_r^{''}$ of the complex dielectric constant. Both α and v are frequency dependent, that express energy absorption and wave dispersion. The impulse response $g(t)$ is determined by petro-physical parameters such as porosity ϕ, density ρ, permeability k_f, grain size KV, water saturation S_W and degree of mineralization S_M, that are of high interest for geologists and geotechnical engineers. Therefore, measurement of the attenuation behavior of EM waves is very suitable to differentiate rocks. For this reason, the determination of both α and v can lead to substantial as well as structural interpretation of certain media. Since the absorption coefficient α of GPR waves in similar to that of seismic waves can be assumed to be linearly frequency-dependent in the first approach, Q-constant hypothesis is valid. The Q factor is inversely

proportional to the absorption coefficient α and therefore describes clearly "material-specific" absorption of different rocks.

Q factor is defined as a measure of the relative energy over a wavelength [1]:

$$\frac{\Delta E}{E} = \frac{2\pi}{Q} \quad \text{..... (1)}$$

or

$$Q = \frac{2\pi}{\Delta E / E} = \frac{2\pi}{(E_1 - E_2)/E_1} \quad \text{.....(2)}$$

Where E_1 as well as E_2 represent mono-frequency energy of EM waves at a distance of wave length λ. Whereas Q values of seismic wave lie in the range 50 – 300, Q values of EM waves lie in the range of 5-80. That means, EM waves are stronger absorbed than seismic waves.

The relation between α and Q is Forkmann and Petzold [2].

$$Q = \frac{\omega}{2v\alpha} \quad \text{.....(3)}$$

As a result, wave function of a plane wave traveling in x direction, which incorporates attenuation can be written as:

$$A = A_0 e^{-\left(\frac{\omega\pi}{2vQ}\right)} e^{j\omega\left(t-\frac{z}{v}\right)} \quad \text{..... (4)}$$

Where A and A_0 denote amplitude at x distance and amplitude at $x = 0, t = 0$, respectively. j is imaginary unit and $j^2 = -1$.

The propagation of electromagnetic waves in geology medium is then characterized by its phase velocity v and Q factor. The measurement of the attenuation behavior of EM waves is very suitable to differentiate rocks. For this reason, the determination (α and v) can lead to substantial as well as structural interpretation .

2. CONSTANT-Q_MODEL AND VELOCITY DISPERSION V(F)

In this study we adopt the so-called Jonscher [3] as the frequency-dependence of the attenuation behavior of geological medium, which is based on the complex permittivity $\bar{\varepsilon}$ or complex dielectric constant $\bar{\varepsilon}_r$ ($\bar{\varepsilon} = \varepsilon_0 \bar{\varepsilon}_r$). The model after Jonscher [3] has a form

$$\bar{\varepsilon} - \varepsilon_\infty = \varepsilon' - \varepsilon_\infty + j\varepsilon'' = \varepsilon_r \left(-j \frac{\omega}{\omega_r} \right)^{n-1} \quad \text{..... (5)}$$

Where 0<n<1, $\omega_r = 2\pi f_r$ and ε_r are all constants and f_r is a certain reference frequency.

The model of a constant Q-value means that the real and imaginary parts of dielectric constant exhibit the same trend of frequency dependency. It is therefore justified to build a complex dielectric constant, whose real- and Imaginary parts appear above a certain peak-frequency in double-logarithmic representation as two parallel lines, as displayed in Figure 2.

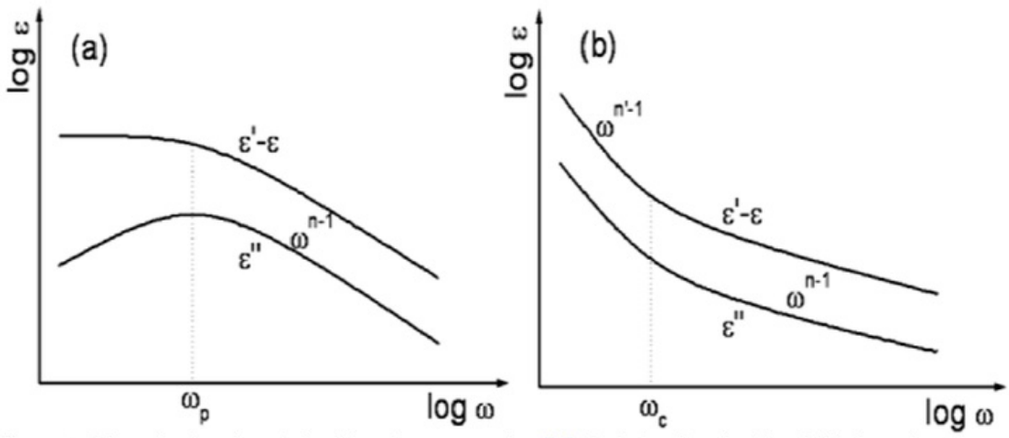

Figure-2. Dispersion function of the dielectric constant after [3]. Both functions in (a) and (b) show the universal behavior at higher frequencies.
(**Source:** Modified by the Researchers)

If we consider only the positive frequencies for the JONSCHER-model (equation 5), we get [4]:

$$\bar{\varepsilon} = \varepsilon_r \left(\frac{\omega}{\omega_r} \right)^{n-1} .\cos\left[\frac{\pi}{2}(1-n) \right] + \varepsilon_\infty + j\varepsilon_r \left(\frac{\omega}{\omega_r} \right)^{n-1} .\sin\left[\frac{\pi}{2}(1-n) \right]. \quad \text{..... (6)}$$

For the relationship between Imaginary and real parts of the above complex permittivity $\bar{\varepsilon}$ it follows:

$$\frac{\varepsilon''}{\varepsilon'} = \frac{\varepsilon_r \sin\left[\frac{\pi}{2}(1-n)\right]\left(\omega/\omega_r\right)^{n-1}}{\varepsilon_r \cos\left[\frac{\pi}{2}(1-n)\right]\left(\omega/\omega_r\right)^{n-1} + \varepsilon_\infty} \quad \ldots\ldots\ldots (7)$$

$$= \frac{1}{Q(\omega)}$$

Equation (7) describes a frequency-dependent Q.

If we define $Q = const. = Q_0$:

$$\frac{1}{Q_0} = \frac{\varepsilon''}{\varepsilon' - \varepsilon_\infty} = \tan\left[\frac{\pi}{2}(1-n)\right] \quad \ldots\ldots\ldots (8)$$

and set $\varepsilon_r' = \varepsilon_r \cos\left[\frac{\pi}{2}(1-n)\right]$ in equation (7) , we get

$$\frac{1}{Q(\omega)} = \frac{\varepsilon_r'\left(\omega/\omega_r\right)^{n-1}}{Q_0\left[\varepsilon_r'\left(\omega/\omega_r\right)^{n-1} + \varepsilon_\omega\right]} \quad \ldots\ldots\ldots\ldots (9)$$

For a weak attenuation or high Q value the dependency of the Q on the frequency can be neglected. Equation (9) can then be approximately written as follows [4]:

$$\frac{1}{Q_C} = \frac{\varepsilon_r'}{Q_0(\varepsilon_r' + \varepsilon_\infty)} \quad \ldots\ldots\ldots\ldots\ldots\ldots (10)$$

Now equation (9) has the same form as the approximation of a constant Q for elastic waves after Putting equation (9) in equation (6) yields

$$\bar{\varepsilon} = \left[\varepsilon_r'\left(\frac{\omega}{\omega_r}\right)^{n-1} + \varepsilon_\infty\right]\left(1 + \frac{j}{Q(\omega)}\right) \quad \ldots(11)$$

The complex wave number $\bar{k}$ can also be written as

$$\bar{k} = \omega\sqrt{\mu\bar{\varepsilon}} = \beta + j\alpha \quad \ldots\ldots\ldots\ldots\ldots (12)$$

Applying equation (9) on equation (12), we get

$$\bar{k} = \omega\left[\mu\varepsilon_r'\left(\frac{\omega}{\omega_r}\right)^{n-1} + \mu\varepsilon_\infty\right]^{1/2}\left(1 + \frac{j}{Q(\omega)}\right)^{1/2} \quad \ldots. (13)$$

Assuming the weak attenuation, the tangent in equation (8) can be approximated with its argument: $\tan\left[\frac{\pi}{2}(1-n)\right] \approx \frac{\pi}{2}(1-n)$.

After some mathematical manipulations (see detail explained in Bano [4] we finally get

$$\bar{k} = \frac{\omega}{v_0}\left[1 - \frac{1}{\pi Q_C}\ln\left(\frac{\omega}{\omega_r}\right) + j\frac{1}{2Q_C}\right] \quad \ldots\ldots\ldots\ldots (14)$$

With $$v_0 = \frac{1}{\sqrt{\mu(\varepsilon_r^{'} + \varepsilon_\infty)}} \quad \ldots\ldots\ldots\ldots\ldots\ldots (15)$$

According to equation (12), equation (14) can be rewritten, so that:

$$\frac{1}{v(\omega)} = \frac{1}{v_0}\left[1 - \frac{1}{\pi Q_C}\ln\left(\frac{\omega}{\omega_r}\right)\right] \ldots\ldots\ldots (16)$$

and $$\alpha = \frac{\omega}{2v_0 Q_C} \quad \ldots\ldots\ldots\ldots\ldots (17)$$

where $\beta = \omega / v(\omega)$.

Equation (16) reflects the dispersion law of velocity by Futtermann [5] for the elastic wave. Equations (15), (16) and (17) describe the relationship between dispersion and absorption

3. IMPULSE RESPONSE

The propagation of electromagnetic (EM) waves in a medium can be considered as a linear system. Figure 3 shows this relation.

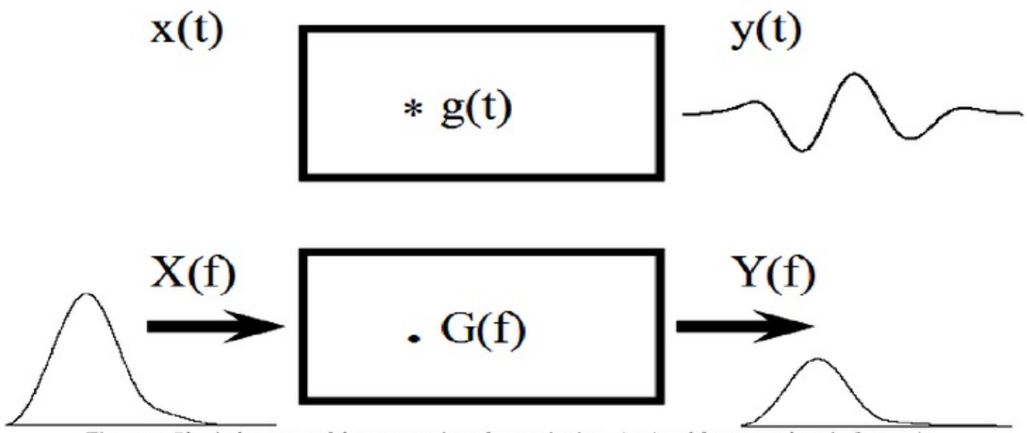

Figure-3. Physical process of the propagation of waves in time- (top) and frequency domain (bottom).
(**Source:** Modified by the Researchers)

The medium is characterized by an impulse response g(t) or its transfer function $G(\omega)$. The output y(t) is resulted from a convolution between the input signal x(t) and the impulse response g(t).

The Fourier transform of the input signal is:

$$X(\omega) = \int_{-\omega}^{\infty} x(t)e^{-j\omega t}\,dt \quad \ldots\ldots\ldots\ldots\ldots (18)$$

If no absorption exists, y(t) can be written as:

$$y(t) = x(t - z/v) = x(t - t_0) \ldots\ldots\ldots\ldots\ldots (19)$$

Where v and t_0 are the propagation velocity of the wave and the travel time, respectively.

According to the shift theorem of Fourier transformation, Fourier transformation of $X(\omega)$ and $Y(\omega)$ differ only with a phase term:

$$Y(\omega) = X(\omega).e^{-j\omega t_0} \quad \ldots\ldots\ldots\ldots\ldots (20)$$

The spectrum of output signal is resulted from a multiplication between the spectrum of input signal $X(\omega)$ and the transfer function $G(\omega)$:

$$Y(\omega) = X(\omega).G(\omega) \quad \ldots\ldots\ldots\ldots\ldots (21)$$

For the transfer function $G(\omega)$ it follows

$$G(\omega) = e^{-\omega t_0} \quad \ldots\ldots\ldots\ldots\ldots (22)$$

For an absorbing medium the transfer function must contain an attenuation term.

Taking the absorption into account, the transfer function becomes **Error! Reference source not found.**:

$$G(\omega) = e^{-\frac{\omega t_0}{2Q}}.e^{-j\omega t_0} \quad \ldots\ldots\ldots\ldots\ldots (23)$$

From equation (20) the impulse response is easily determined through its inverse Fourier transformation

$$g(t - t_0) = \frac{t_0/2Q}{(t_0/2Q)^2 + (t - t_0)^2} \quad \ldots\ldots\ldots\ldots (24)$$

It can be seen from the course of the impulse response in Figure 3 that it is about a Lorentz curve whose maximum lies at $t = t_0$ and symmetrical about earlier and later times. The propagation of EM waves must be described by physically realizable process, where the causality principle applies. Therefore, for t < 0 the impulse response function must disappear. It requires a correction in equation (23). This is achieved by introducing velocity dispersion in equation (23), where higher frequencies travel faster than the lower ones .

For the mathematical description of this under linear dispersion function there are a number of different approaches. In the present work, the Dispersion relation after Futtermann [5] is used:

$$v(\omega) = v(\omega_0)\left[1 - \frac{1}{\pi Q}\ln\left(\frac{\omega}{\omega_r}\right)\right]^{-1} \quad \ldots\ldots (25)$$

or $$\frac{1}{v(\omega)} = \frac{1}{v(\omega_0)}\left[1 - \frac{1}{\pi Q}\ln\left(\frac{\omega}{\omega_r}\right)\right] \quad \ldots\ldots (26)$$

Where $\omega = 2\pi f_0$ is a frequency reference.

Put equation (26) into equation (23):

$$G(\omega) = e^{-\frac{\omega t_0}{2Q}} . e^{-j\omega t_0\left[1 - \frac{1}{\pi Q}\ln\frac{\omega}{\omega_0}\right]} \quad \ldots\ldots\ldots (27)$$

or $$G(\omega, t_0) = A(\omega, t_0)e^{jP(\omega, t_0)} \quad \ldots\ldots\ldots (28)$$

with

$$A(\omega, t_0) = e^{-\frac{\omega t_0}{2Q}} \quad \ldots\ldots\ldots\ldots\ldots (29)$$

$$P(\omega, t_0) = -\omega t_0 - \phi(\omega, t_0) \quad \ldots\ldots\ldots\ldots (30)$$

$$\phi(\omega, t_0) = -\frac{\omega t_0}{\pi Q}\ln\frac{\omega}{\omega_0} \quad \ldots\ldots\ldots\ldots (31)$$

Equation (29) and equation (30) represent amplitude spectrum and phase spectrum, respectively.

The reference frequency ω_0 occurs only in phase spectrum and for our purpose in this work we use NYQUIST frequency as the reference frequency: $\omega_0 = \omega_{NY}$. Thus, it appears finally to the transfer function of absorbing medium with causal impulse response

$$G(\omega) = e^{-\frac{\omega t_0}{2Q}} . e^{-j\omega t_0\left[1-\frac{1}{\pi Q}\ln\frac{\omega}{\omega_{NY}}\right]} \quad \ldots\ldots\ldots(32)$$

or $$G(\omega) = e^{-\frac{\omega t_0}{2Q}} . e^{-j\omega t_0} e^{j\frac{\omega t_0}{\pi Q}\ln\frac{\omega}{\omega_{NY}}} \quad \ldots\ldots\ldots\ldots (33)$$

In equation (33) the first term represents the absorption factor, the second term the travel time factor and the third term the Dispersion factor. Figure 4 shows the influence of Q factor on the course of amplitude as well as phase spectra. The figure demonstrates that absorption and dispersion effect increases with decreasing Q.

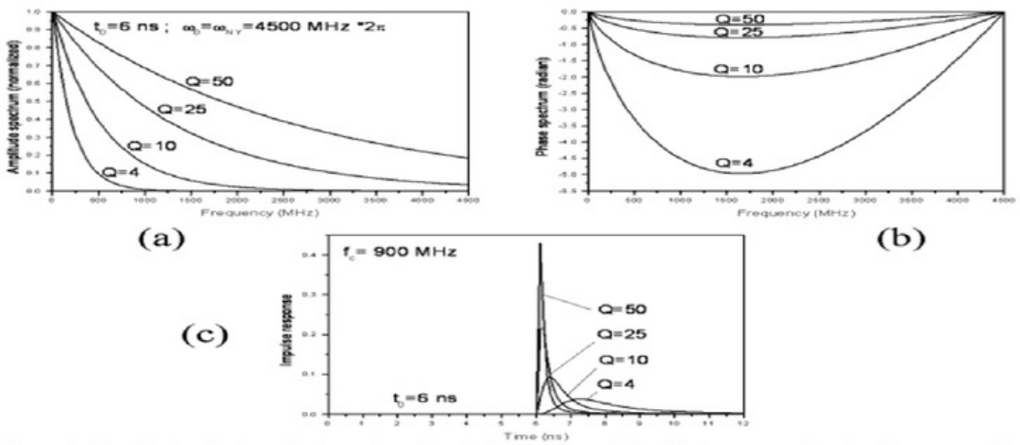

Figure-4. Transfer function (amplitude spectrum (a) and phase spectrum (b) and their corresponding impulse response (c). parameter: Q factor. Model input: t_0 = 6 ns, $\omega_0 = \omega_{NY}$ and f_c = 900 MHz.
(**Source:** Data Processing by the Researchers)

4. FORWARD MODELING AND ABSORPTION DETERMINATION

As illustrated in Figure 4, propagation of electromagnetic (EM) waves in a medium is described as linear system through this relation:

$$y(t) = x(t) * g(t) \quad \ldots\ldots\ldots\ldots\ldots\ldots (34)$$

By using equation (32) we carried out forward modeling using input data listed in Table 1.

Table-1. Data For Forward Modeling

Case	Input signal $x(t)$	Travel time t_0 in ns
1	Model signal A (900 MHz)	3
2	Model signal A (900 MHz)	6
3	Model signal A (900 MHz)	9
4	Model signal A (900 MHz)	12
2b	Model signal A (900 MHz)	6
4b	Model signal A (900 MHz)	12

(**Source:** Parameters by the Researchers)

The model wavelet A and B are the extracted wavelets, which are obtained from the measurement in the air with 900 MHz and 450 MHz antennas frequency, respectively. The impulse response is determined by using inverse Fourier transformation (IFT) of the transfer function:

$$g(t) \xleftarrow{IFT} G(\omega) \quad \ldots\ldots\ldots\ldots\ldots\ldots\ldots\ldots (35)$$

The transfer function $G(\omega)$ is calculated using equation (33). It describes filter properties of medium in frequency domain. Its input parameters are travel time t_0 and Q factor.

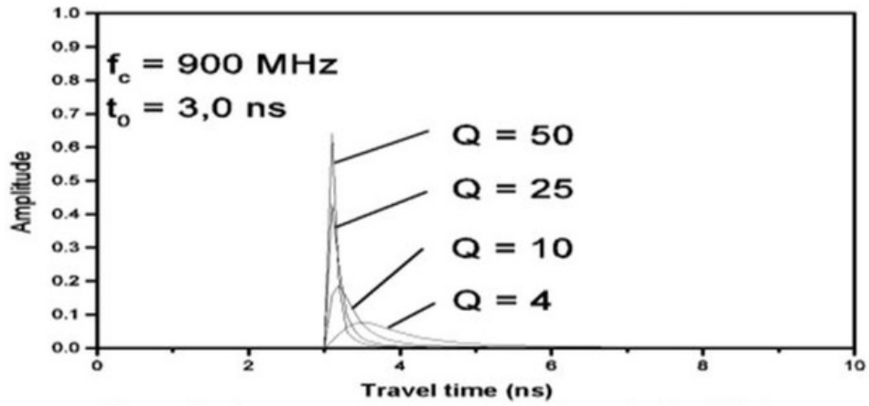

Figure-5. Impulse response at the same travel time t_0 (t_0 = 3 ns) with variable Q
(**Source:** Data Processing by the Researchers)

Figure 5 shows various impulse responses at the same travel time t_0 (t_0 = 3 ns). It can be seen, that for small Q (high attenuation) the impulse response becomes smaller and wider. A smaller impulse response means that more energy is absorbed. A wider impulse response means, that more time is required to transfer the energy of EM waves. That means also, that the main energy is transferred in later time.

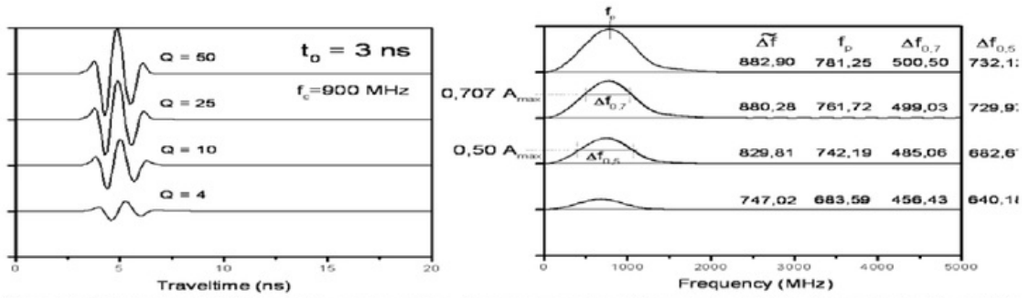

Figure-6. Output signal (left) and their corresponding frequency spectra at the same travel time t_0 (t_0 = 3 ns) with variable Q.
(**Source:** Data Processing by the Researchers)

Figure 6 represents the output signal and its corresponding frequency spectrum at the same travel time t_0 (t_0 = 3 ns) but with different Q. With decreasing Q value the output signal becomes smaller and wider. Its peak frequency increases and shifts to lower frequency. It also applies to impulse responses as well as output signals at the same Q value (Q=50) with decreasing t_0 (see figure 7 and 8).

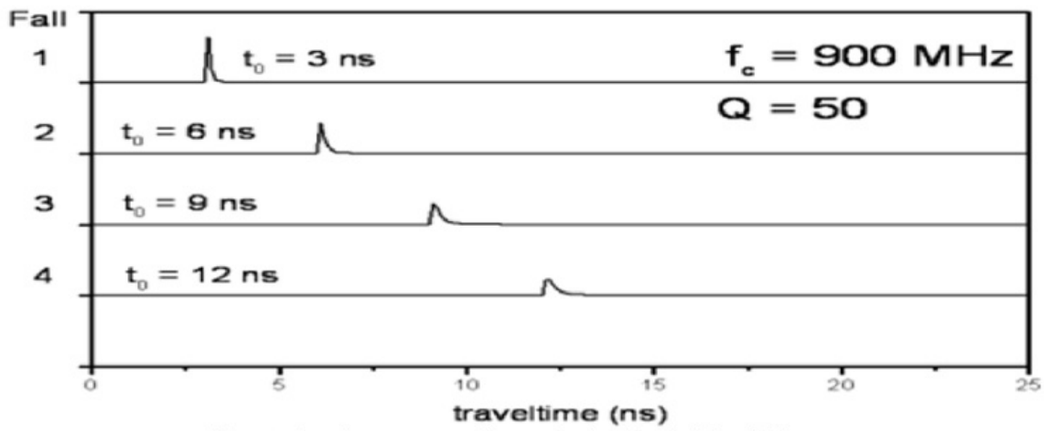

Figure-7. Impulse responses at the same Q value (Q-50) with variable t_0
(**Source:** Data Processing by the Researchers)

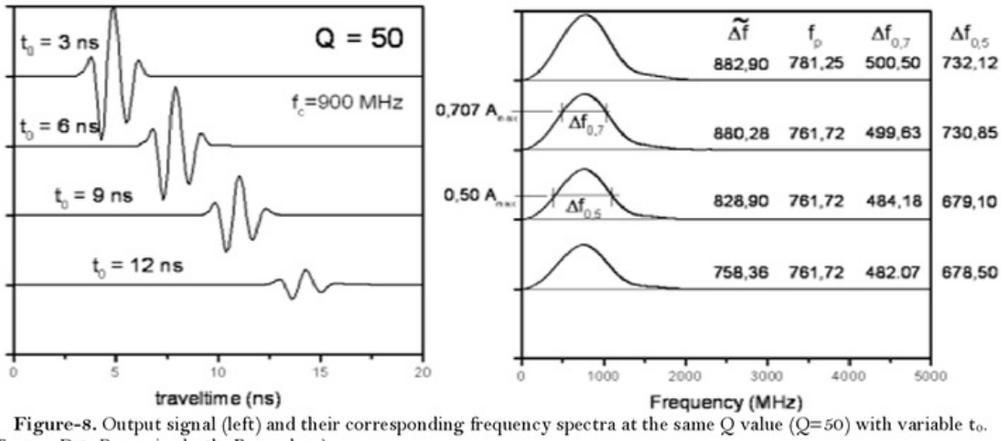

Figure-8. Output signal (left) and their corresponding frequency spectra at the same Q value (Q=50) with variable t_0.
(**Source:** Data Processing by the Researchers)

With increasing t_0 the impulse response becomes smaller and wider. That means EM waves at the same Q are more attenuated as they propagate at longer distance. The transferred energy is lower, and the main energy will be later transferred. With increasing t_0 the peak frequency shifts to lower frequency.

In Figures 6 and 8 the characteristic frequencies are listed: the equivalent bandwidth $\tilde{\Delta f}$, peak-frequency f_P, the bandwidth at 0.70 maximum amplitude $\Delta f_{0.7}$ and the bandwidth at 0.5 maximum amplitude $\Delta f_{0.5}$. It shows that the higher the Q value at the same travel time as well as the longer the travel time at the same Q is, the smaller the corresponding band-width as well as the peak frequency is.

Q values are determined from the ratio between the two signals or their frequency spectra.

The easiest way to Q-determination is the so-called Amplitude decay method. From the relationship between the amplitude for two different distances x_1 and x_2 as well for times $t_1 = x_1 / v$ and $t_2 = x_2 / v$ t2:

$$Q = \frac{\pi f \Delta x}{v} \ln\left[\frac{a(x_1)}{a(x_2)}\right] = \pi . f . t_0 \ln\left[\frac{a(x_1)}{a(x_2)}\right] \quad \text{.....(34)}$$

With f as the dominant frequency and $t_0 = t_2 - t_1$ as the travel time. $a(x_1)$ and $a(x_2)$ are the signal amplitudes at x_1 as well x_2. This method has disadvantage that it can only be applied if true amplitudes exist. The dominant frequency or apparent frequency gives us only an estimate value.

The second technique is the so-called spectral ratio method. This technique is probably the well-known method for the determination of Q. With this method the absorption effects are determined in frequency domain. It is based on the building of the Amplitude spectral ratio of two signals. This method was extensive described in the works of Doan [6]. Therefore this procedure is here briefly explained and is directly described for the case of transmission signals.

If we build the ratio of amplitude spectra of two different signals and we calculate its logarithmic value, the ratio of the corresponding Futterman's transfer function arises to

$$\ln \frac{|Y(f)|}{|X(f)|} = const. - \frac{\Delta t \pi f}{Q} \quad \text{.....(35)}$$

Where Δt denotes the travel time difference between $y(t)$ and $x(t)$.

Q is determined from the slope of the linear function in the frequency-dependence at a distinct travel time difference (see figure 9).

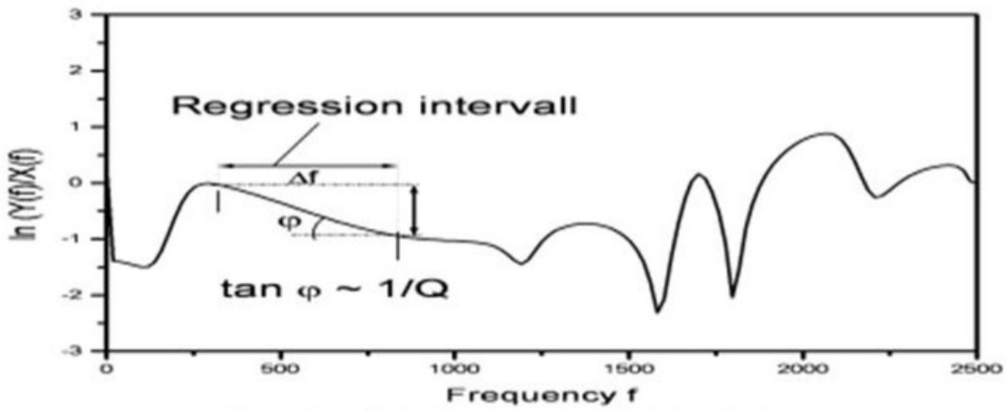

Figure-9. Logarithmic values of spectral ratio for Q determination
(**Source:** Data Processing by the Researchers)

Q-factor is inversely proportional to the angle ϕ: $\tan\phi \propto 1/Q$. A general problem that exists in the Q-determination with this method is in estimating frequency intervals.
Absorption coefficient α is determined from two different signals:

$$\alpha = \frac{1}{x_2 - x_1} \ln \frac{a(x_1)}{a(x_2)} \quad \ldots\ldots\ldots\ldots\ldots\ldots (36)$$

or

$$\alpha = \frac{1}{x_2 - x_1} .20.\log \frac{a(x_1)}{a(x_2)} \quad \ldots\ldots\ldots\ldots (37)$$

α in equation (36) has a unit of Neper/m, whereas α in equation (37) dB/m. Using equation (36), Q is then calculated using equation (3).

5. INVESTIGATION ON REAL DATA

The validity of three methods for Q determination, namely spectral ratio and amplitude decay methods as well as method for Q determination over α , was tested on real data. One dataset is available for the investigation: transmission measurement data acquired on existing gneiss body. The measurement is conducted with pulse Ekko-1000 GPR system with 900 MHz and 450 MHz nominal frequency. Low pass-filter with higher frequency cut-off of 0.3 f_{NY} was applied on all data. The empirical signal extracted from measurement in the air was utilized.

Gneiss as a crystalline rock is selected as an ideal test medium due to its small absorption and therefore resulting in large depth penetration. The object is located in "Reiche Zeche" Schacht, in Saxony State of Germany, at a depth of 180m (Fig. 10).

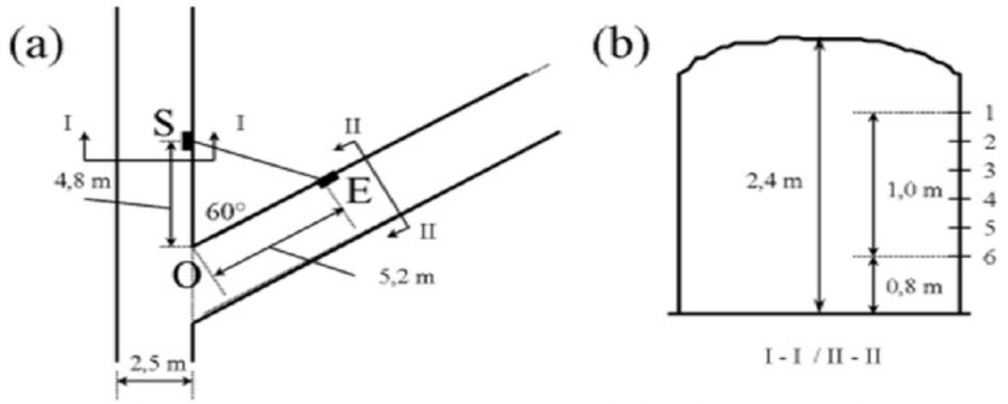

Figure-10. Sketch of test site (a) and cross section I - I as well as II - II (b). S and E are the position of transmitting- and receiving antenna, respectively.
(**Source:** Layouts by the Researchers)

The test object is selected so that it represents a quasi-homogeneous medium. The Gneiss wall is not flat, therefore it was difficult to stand the antenna surface on the Gneiss wall to position, so that parallel antennas are guaranteed. In spite of this handicap, the transmission signal could be received relatively good. Contrary from this condition, the recorded signals at horizontal measurement were so bad that only a few trace can be analyzed.

Two different measurement configurations were realized (see Figure 8). Two different measurement configurations were implemented (see Figure 10). In horizontal measurement, transmitter and receiver antennas at a height of about 120cm to 150cm from O to S as well as from O to E were synchronizingly moved with 0.5m step forward. Vertical measurement means that the antennae were synchronizingly moved vertically from top to bottom with 20cm step. Figures 11 and 12 are the results with the 900 MHz antennas for the horizontal as well as vertical measurements, It is concluded from the measurement data that in particular with the 450 MHz antennas the recorded transmission signals sufficiently appear only at a larger transfer distance. Therefore, only the measurements with the 900-MHz-antennas are introduced. In addition to absorption determination, velocity value is also calculated.

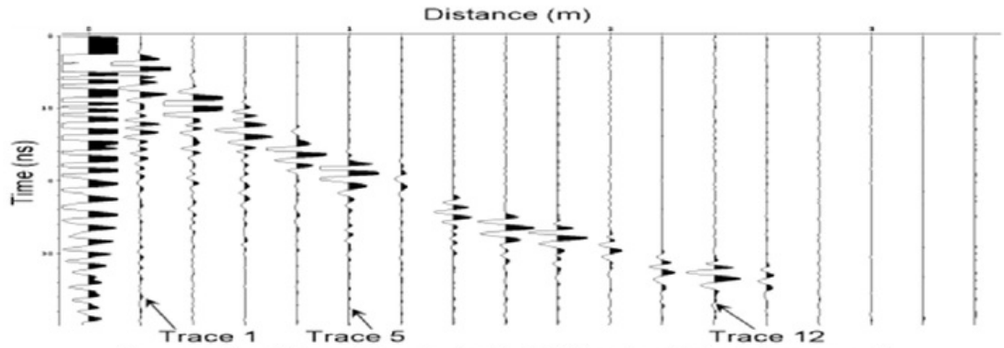

Figure-11. Recorded transmission signals with 900 MHz antenna (horizontal measurement)

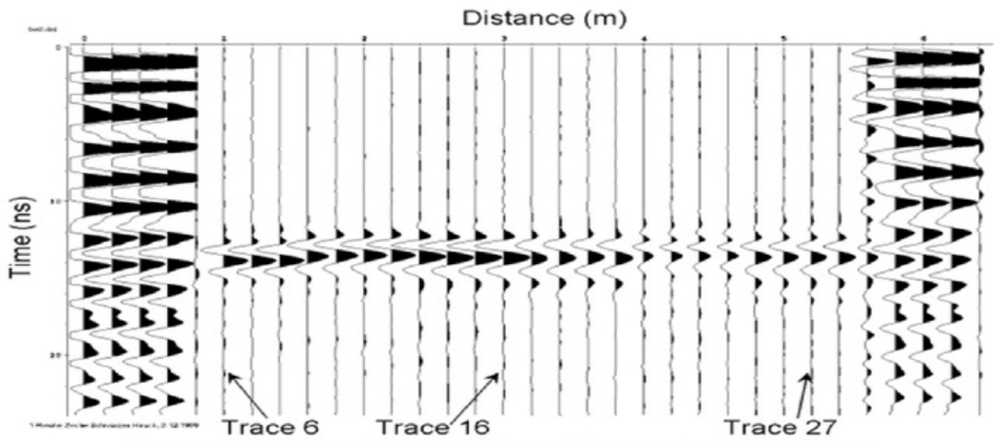

Figure-12. Recorded transmission signals with 900 MHz antenna (vertical measurement)
(**Source:** Data Processing by the Researchers)

In order to obtain velocity and absorption from horizontal measurement, trace numbers 5, 8, 9 and 12 are used (see Figure 11). The important data are summarized in Table 2.

Table-2. Important Data Extracted From Trace 5, 8, 9 and 12

Trace	t_0 (ns)	v (m/ns)	f_{peak} (MHz)
5	17.0	17.12	624.99
8	24.3	17.74	585.93
9	26.1	18.31	585.63
12	31.6	18.53	484.36

(**Source:** Parameters by the Researchers)

Traces 4 and 5 are available for the input signal. Since amplitudes of trace 5 are higher than those of trace 4, signal from trace 5 is chosen as input signal. For Q determination signals from traces no. 8, 9 and 12 are considered as output signals. Using equations (34) and (35) , Q values are determined and their results are listed in Table 3.

Table-3. The Result of the Q Determination Using 2 Methods for Horizontal Measurement

Input signal	Output signal	Δt_0 (ns)	Calculated Q	
			Amplitude decay	Spectral ratio
Trace 5	Trace 8	7.3	38.80	40.70
Trace 5	Trace 9	9.1	38.62	40.17
Trace 5	Trace 12	14.6	44.23	45.72

(**Source:** Results by the Researchers)

Three different trace Q-values of more than 40 are delivered. The same traces are used to calculate their absorption coefficient using equation (37) and Q values using equation (3). Velocity value listed in Table 2 is used for Q computation. The results are summarized in Table 4.

Table-4. The Result of the Q Determination from a for Horizontal Measurement

Input signal	Output signal	α in dB/m	Calculated Q
Trace 5	Trace 8	2.058	43.80
Trace 5	Trace 9	1.852	41.14
Trace 5	Trace 12	1.729	46.57

(**Source:** Results by the Researchers)

From Tables 5 and 6, it is concluded that the calculated Q data meet good agreement, where the determined Q-values lie between 40.166 and 46.57.

Table-5. The Result of the Q Determination Using 2 Methods Vertical Measurement

Input signal	Output signal	t_0 (ns)	Calculated Q	
			Amplitude decay	Spectral ratio
Trace 5	Trace 9	27.7	32.39	33.45
Trace 5	Trace 10	27.6	32.52	33.58
Trace 5	Trace 11	27.6	32.64	33.71
Trace 5	Trace 12	27.6	32.79	33.85
Trace 5	Trace 13	27.7	33.84	34.95
Trace 5	Trace 14	27.8	33.96	35.07
Trace 5	Trace 15	27.8	33.87	34.96
Trace 5	Trace 16	27.7	34.31	35.43
Trace 5	Race 27	27.9	31.07	32.11

(**Source:** Results by the Researchers)

Table-6. The Result of the Parameter Determination V and A as Well as Q For Gneiss

No.	v (m/ns)	α (dB/m)	Q	fc (MHz)	Depth (m)	Source
1	0.17 - 0.18	1.7 - 2.1	30 - 46	900	180	This study
2	0.10 - 0.12					Grasmueck [7]
3	1.12 - 0.12			100	Up to 30	
4	0.17	2.6				
5	0.12	6.9				
6	0.17	1.5 – 4.5	30	300 - 900		
7	0.13	9.0 – 27.0	7			
8	0.08-0.11					

(**Source:** Results by the Researchers)

We obtain similar results with vertical measurement (see Figure 12). From three different methods to Q-determination, the calculated Q-values lie on about 32 in average.

Comparing the results of both the horizontal and vertical measurements, approximately 20% difference exists. Possible cause for this is the orientation of the receiving antenna during the measurement. In the vertical measurement the orientation of the antenna at the vertical positions agrees well, at which every position was measured three times. That was not so at the horizontal

measurement. The results of both measurement, which are compared with the data from the literature are listed in Table 10.

6. CONCLUSION

Propagation of electromagnetic waves is described by two parameters, namely phase velocity v and absorption coefficient α as well as Q factor. Both are the most important parameters for the processing and interpretation of Ground-penetrating radar (GPR) data. These propagation parameters are frequency-dependent, which describe the wave attenuation during their propagation in absorbing medium. This attenuation process results in energy absorption and wave dispersion. From the linear basis of the frequency dependence of α of geology medium, a constant Q-hypothesis is applied, whereby the Q factor is inversely proportional to α and describes degree of absorption of distinct rocks. Theoretical and practical considerations for the propagation of electromagnetic waves in absorbing Medium lead to the use of a model with constant Q and velocity dispersion

Forward modeling with such considerations was carried out, so that the propagation of electromagnetic waves in absorbing medium can be described as approximating the real condition. On the basis of such model, the effect of these parameters on wavelets is investigated. Attenuation process causes the wave amplitudes smaller with increasing distance at the same Q and causes the wave amplitudes smaller with decreasing Q at the same distance (absorption) and the waveforms are stretched (dispersion). The longer the distance at the same Q as well as the smaller Q at the same distance, the smaller is the bandwidth of the transmission wavelets. Its peak frequency shifts to lower frequencies. Three methods for Q determination are reviewed, namely spectral ratio and amplitude decay methods as well as Q-determination method through α- determination. The three methods are then applied on real data, which are acquired from transmission measurement at test site in Reiche Zeche Shaft in Germany. This study shows that Q determination using the three methods is successfully applied on real transmission data. This work suggests us to extend the use of the methods to reconstruct tomographically the distribution of Q in medium.

7. ACKNOWLEDGMENTS

The authors wish to express their gratitude to the Department of Geophysical Science & Engineering, ITB and University of Sriwijaya for the support during the development of this research, and Faculty of Engineering Sriwijaya University for the support to fund this research, and sponsors.

REFERENCES

[1] D. H. Johnston and M. N. Toksoz, "Definitions and terminology.- In: Toksoz M.N., Johnston D.H., eds., Seismic wave attenuation.- SEG," *Geophysics Reprint Series*, vol. 2, pp. 1-5, 1981.

[2] B. Forkmann and H. Petzold, *Prinzip und anwendung des gesteinsradars zur erkundung des nahbereiches* vol. 432. Leipzig: VEB Deutscher Verlag für Grundstoffindustrie, 1989.

[3] A. K. Jonscher, "The, universal dielectric response," *Nature*, vol. 267, pp. 673-679, 1977.

[4] M. Bano, "Constant dielectric losses of ground-penetrating radar waves," *Geophys J. Internat*, vol. 124, pp. 279 – 288, 1996.

[5] W. I. Futtermann, "Dispersive body waves," *J. Geophys. Res.*, vol. 67, pp. 5279-5291, 1962.

[6] D. Doan, "Untersuchungen zur absorption seismischer Wellen mit der spektrendivisions-und der phasendifferenzmethode," PhD Thesis, TU Braunschweig, 1984.

[7] M. P. Grasmueck, "3-D ground-penetrating radar applied to fracture imaging in gneiss," *Geophysics*, vol. 61, pp. 1050-1064, 1996.

Q DETERMINATION OF TRANSMISSION GPR WAVES IN ABSORBING MEDIA

ORIGINALITY REPORT

7%	%	7%	%
SIMILARITY INDEX	INTERNET SOURCES	PUBLICATIONS	STUDENT PAPERS

PRIMARY SOURCES

1	Ikponmwosa, Oghogho, Frederick O. Edeko, and Joy Emagbeter. "Measurement and modelling of TCP downstream throughput dependence on SNR in an IEEE802.11b WLAN system", 2016 Annual Conference on Information Science and Systems (CISS), 2016. Publication	3%
2	Parnadi, Wahyudi Widyatmoko (and TU Bergakademie Freiberg, Geowissenschaften, Geotechnik und Bergbau). "Kennwert-Schätzung aus Georadar-Transmissionsdaten", Technische Universitaet Bergakademie Freiberg Universitaetsbibliothek "Georgius Agricola", 2009. Publication	1%
3	Won Young Yang. "Signals and Systems with MATLAB", Springer Nature, 2009 Publication	1%
4	Neal, A.. "Ground-penetrating radar and its use in sedimentology: principles, problems and progress", Earth Science Reviews, 200408 Publication	<1%
5	Lear, Caroline H., Helen K. Coxall, Gavin L. Foster, Daniel J. Lunt, Elaine M. Mawbey, Yair Rosenthal, Sindia M. Sosdian, Ellen Thomas, and Paul A. Wilson. "Neogene ice volume and ocean temperatures: Insights from infaunal foraminiferal Mg/Ca paleothermometry :	<1%

NEOGENE MG/CA PALEOTHERMOMETRY", Paleoceanography, 2015.
Publication

---

6 Marcillo, Omar, Stephen Arrowsmith, Philip Blom, and Kyle Jones. "On infrasound generated by wind farms and its propagation in low-altitude tropospheric waveguides : WIND-FARM INFRASOUND IN THE TROPOSPHERE", Journal of Geophysical Research Atmospheres, 2015. <1%
Publication

---

7 Ansam Subhi Jabbar, Ali Kareem Nahar, Hussain Kareem Khleaf, Mohammed Jawed Mortada. "Modified Local Search Particle Swarm Optimization Algorithm Based on Channel Estimation with VHDL", 2018 Third Scientific Conference of Electrical Engineering (SCEE), 2018 <1%
Publication

---

8 Valek, P. W., J. Goldstein, J.-M. Jahn, D. J. McComas, and H. E. Spence. "First joint in situ and global observations of the medium-energy oxygen and hydrogen in the inner magnetosphere. : MEDIUM ENERGY H AND O OBSERVATIONS", Journal of Geophysical Research Space Physics, 2015. <1%
Publication

---

9 Norbert Blindow. "Ground Penetrating Radar", Environmental Geology, 2008 <1%
Publication

---

10 Norman Wagner. "Determination of the spatial TDR-sensor characteristics in strong dispersive subsoil using 3D-FEM frequency domain simulations in combination with microwave dielectric spectroscopy", Measurement Science and Technology, 04/01/2007 <1%

Publication

11	Lanbo Liu, John W. Lane, Youli Quan. "Radar attenuation tomography using the centroid frequency downshift method", Journal of Applied Geophysics, 1998 Publication	<1%
12	Tina Wunderlich, Wolfgang Rabbel. "Attenuation of GPR waves in soil samples based on reflection measurements", 2011 6th International Workshop on Advanced Ground Penetrating Radar (IWAGPR), 2011 Publication	<1%
13	"Emerging Research in Artificial Intelligence and Computational Intelligence", Springer Science and Business Media LLC, 2012 Publication	<1%

Exclude quotes	On	Exclude matches	< 5 words
Exclude bibliography	On		